Supporting Information

Ultrathin Two-Dimensional Polydopamine Nanosheet for Free Radical Scavenging and Wound Healing

Yasun Jing[a], *Zhenru Deng*[a], *Xiuyun Yang*[a], *Leijiao Li*[a,*], *Ying Gao*[a,*] *and Wenliang Li*[b,*]

1. Materials

Dopamine hydrochloride, riboflavin and methionine (Met) paraformaldehyde purchased from Aladdin Reagent (Shanghai) Co., Ltd.; 1,1-diphenyl-2-picrylhydrazyl (DPPH) , 2,2'-azino-bis(3-ethlbenzothiazoline-6-sulfonic acid) diammonium salt (ABTS), potassium persulfate ($K_2S_2O_8$) and nitrogen blue tetrazolium (NBT) were purchased from Macklin Co. LLC.; Ethylenediaminetetraacetic acid (EDTA) was bought from Tianjin Guangfu Technology Development Co., Ltd.; Trypsin (0.25%)-EDTA solution was purchased from Beijing Solarbio Science & Technology Co., Ltd.; DMEM medium was purchased from Hyclone; Fetal bovine serum (FBS) was purchased from Zhejiang Tianhang Biotechnology Co., Ltd.; Double antibody (penicillin + streptomycin) was purchased from Gibco; dimethyl sulfoxide (DMSO) was purchased from Beijing Dingguo Changsheng Biotechnology Co., Ltd.; MTT reagent was purchased from Sigma-Aldrich, Pentobarbital sodium was bought from Sinopharm Chemical Reagent Co., Ltd.. In this study, the solvents used to prepare the solution were methanol, 95% ethanol, tri-distilled water and PBS. Beyond that, 75% ethanol and normal saline were also used during the experiment. Healthy male SD rat weighing about 220g (SPF grade, 6-8 weeks old) from Liaoning Changsheng Biotechnology Co., Ltd. All animal experiments, including animal care, dosing, and termination, were performed according to the guidelines of the local Animal Ethics Committee of Changchun University of Science and Technology.

2. Experimental Section

2.1 Preparation of PDA NSs

Briefly, dopamine hydrochloride was used as the precursor to directly synthesize PDA NSs via a self-assembly reaction route. 200 mg of dopamine hydrochloride was dissolved in 90 mL of tri-distilled water at pH 6.8. The mixture solution was then reacted at 50 °C with vigorous stirring for 24 hours. As the reaction time progresses, the color of the solution gradually changed from pale pink to earth-yellow. Afterward, centrifugation strategy of "liquid cascade centrifugation" (LCC) was carried out to obtain PDA NSs. The resulting earth-yellow solution was centrifuged under different centrifugal speeds for 10 min to remove the larger size of the material. The specific centrifugation operation steps were as follows. At step one, the precipitate was discarded and the supernatant was reserved after centrifuging at 500 rpm and the morphology of the supernatants was shown in Figure S1a. Then, the collected supernatant was centrifuged at 1000 rpm again and the morphology of the supernatants was presented in Figure S1b. Finally, the supernatant collected in the previous step was further centrifuged at 1500 rpm. The precipitate was illustrated in Figure S1c. And the supernatant were collected for experiments.

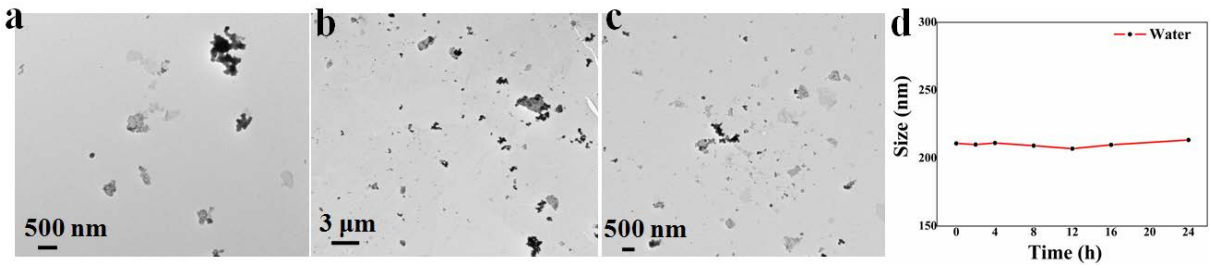

Figure S1. a-c)The TEM of products under different centrifugal speeds; d) Stability of PDA NSs in water, by monitoring the nanosheet size in 24 hour;

Fourier transform infrared spectra and ^{13}C NMR of PDA nanoparticles (PDA NPs) and PDA NSs were provided in Figure S2. Compared the FTIR spectrum of dopamine monomer and PDA nanoparticles (PDA NPs) [1-2], PDA NSs exhibited narrow peaks at

1,519, 1,340, 1,322, 1,190 and 1,175 cm^{-1}, which attributed to NH_2 scissoring vibration, CH_2 bending vibration, C-O-H bending vibration, C-O symmetry vibration, and C-C stretching vibration modes, respectively. In contrast, the conventional PDA NPs showed the a large and broad peak spanning 1,500-1,000 cm^{-1}. ^{13}C NMR spectra of PDA NSs obtained after lyophilization showed sharp peaks at 42 ppm attributed to the aliphatic species..

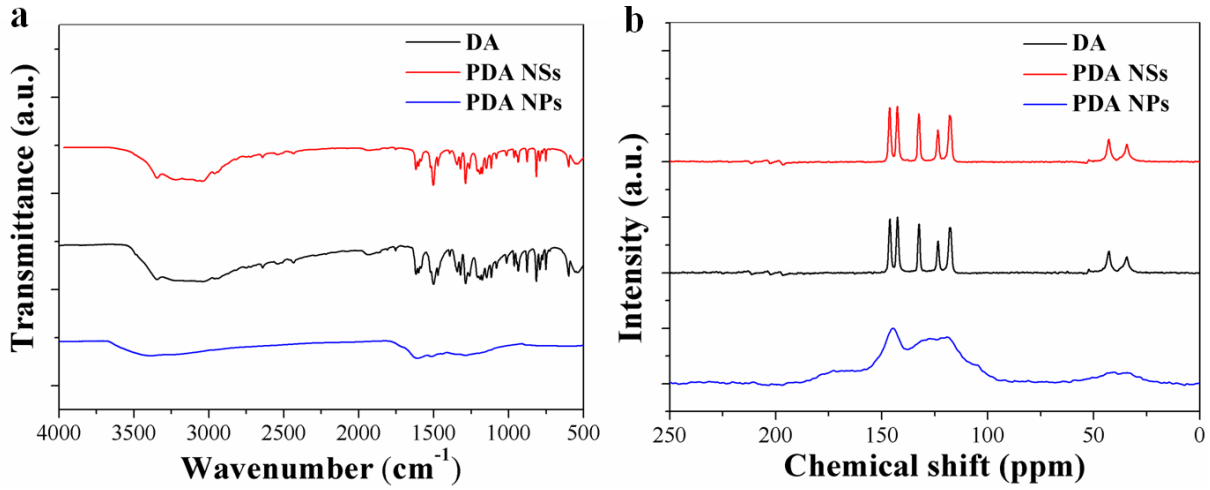

Figure S2. a) FTIR spectra and b) ^{13}C NMR spectra of DA, PDA NPs and PDA NSs

2.2 DFT calculations

The structure of single DHI molecule was optimized with density functional theory (DFT) employing the B3LYP exchange–correlation functional with the Pople's allelectron basis set 6-31+G(d) as implemented in the Gaussian09 program [3-5]. Weak interactions were determined by semi-empirical PM6-D3H4 method using Mopac2012 program [6].

Moreover, DFT calculations were performed to figure out the array of the microstructure units and the week interaction within these PDA NSs as complementary. From the inspiration of common formation of polydopamine, the dopamine was considered to rearrange into 5,6-dihydroxyindole (DHI) at first. Thereafter, DHI could easily form trimeric conjugated crosslinked polymers (TDHI). Finally, polydopamine could be held together through strong non-covalent forces.

The theoretical results revealed that the 2D layer framework was also held together with weak interaction, which was consistent with that reported in previous paper. The hydrogen bonding within one layer and π-π stacking between interlayer is well demonstrated in Figure S6. Initially, we optimized the DHI and the calculated length, width and height were 1.7, 1.4, 0.8 nm, respectively (Figure S3a). The volume of two sets of TDHI was illustrated in Figure S3b. The definite hydrogen bonding was found between hydrogen atom belonging to one set of TDHI and the oxygen atoms attaching to another set of TDHI in the same layer, which were presented as blue fragments as demonstrated in Figure S3c. To minimize the computational cost, the interactions were estimated within six sets of TDHI, which arranged in two layers with the interlayer distance of about 3.4 Å. The π-π stacking was clearly displayed as blue-green fragments resulting in arranging layers together as presented in Figure S3d.

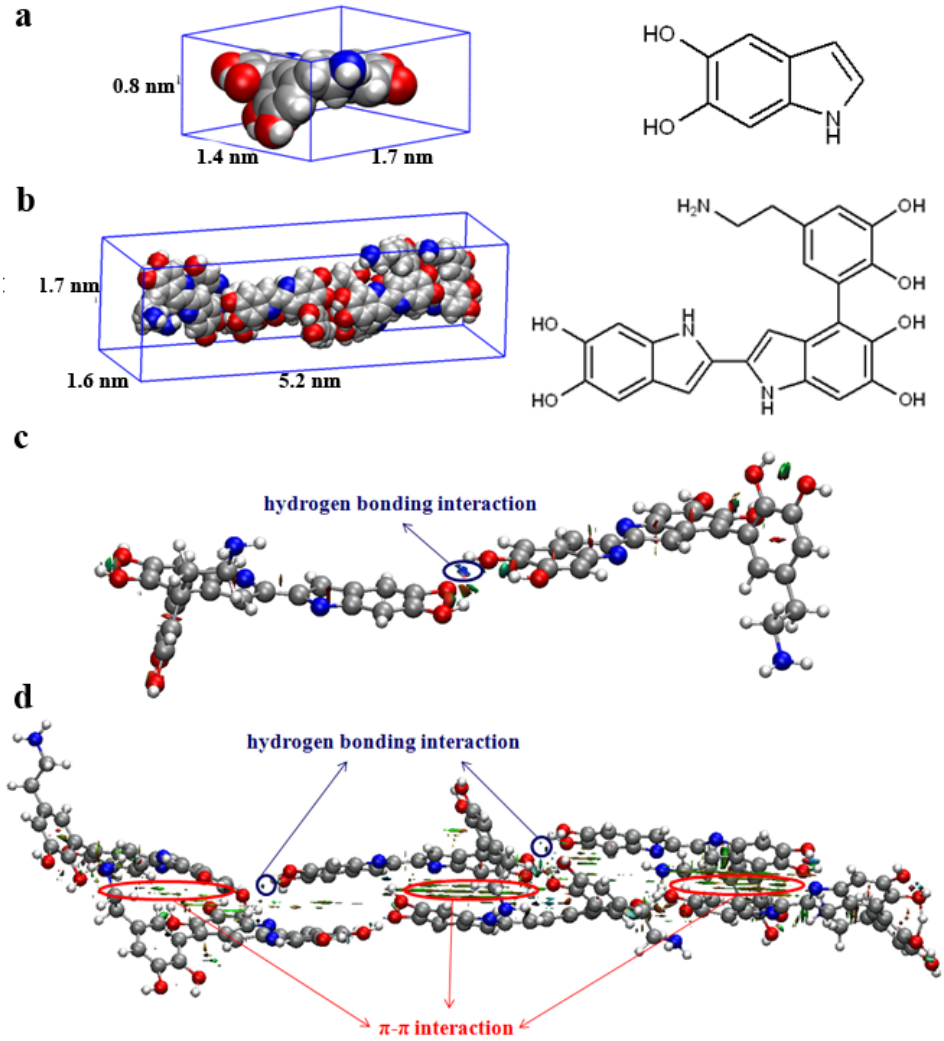

Figure S3 (a) The volume and the structure of single DHI molecule; (b) The volume of two TDHI molecules and the structure of TDHI molecule; (c) The intermolecular forces between two sets of TDHI; (d) The intermolecular forces between six sets of TDHI molecules. Low-gradient isosurfaces (s = 0.5 au) were generated by program Multiwfn through the popular visualization software VMD. The surfaces are colored on a blue-green-red scale according to values of sign(λ_2)ρ, ranging from -0.04 to 0.02 au.

2.3 Scavenging of $O_2^{\cdot -}$

The scavenging rate (Y) of $O_2^{\cdot -}$radicals by PDA NSs was calculated according to Formula S1.

$$Y = [1-(A_0-A_n/A_P-A_n)]\times 100\% \quad (S1)$$

where A_p is the absorbance at 560 nm of the mixture containing 2 μM riboflavin, 13 mM methionine, 75 μM NBT, 100 μM EDTA without PDA NSs under illumination (positive

control group), A_n is the absorbance at 560 nm of the mixture in dark (negative control group), A_0 is the absorbance at 560 nm of the mixture and PDA NSs with different concentration under illumination.

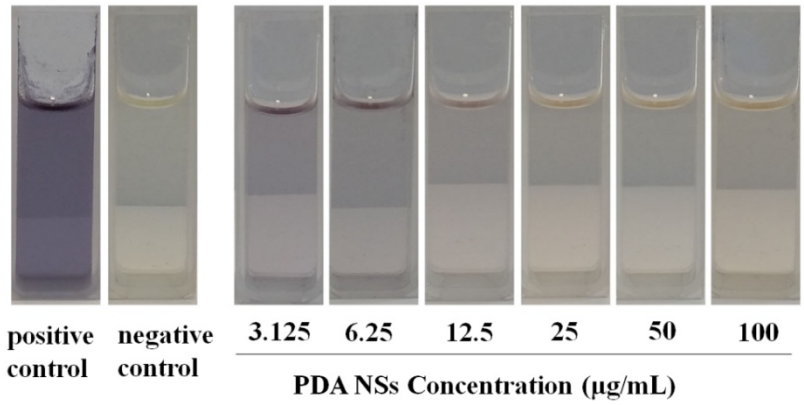

Figure S4. Color variations in $O_2^{\cdot -}$ free radical scavenging test.

2.4 Scavenging of DPPH·

DPPH can be well dissolved in methyl alcohol with the density of 45.6 μg mL^{-1}. In the presence of antioxidants, the DPPH· free radical with a free electron on its nitrogen atom accepts one electron from antioxidants to form the non-radical DPPH-H, resulting in the color of DPPH solution fading from purple to faint yellow (**Figure S5**). Fortunately, the prepared PDA NSs also have good dispersion in methyl alcohol. The free radical scavenging rate (Y) of DPPH· was calculated according to Formula S2 and the average value was taken.

$$Y=[1-(A_s-A_r)/A]\times 100\% \quad (S2)$$

where A is the absorbance of the mixture containing 5 mL DPPH and 1 mL 95% ethanol without PDA NSs, A_r is the absorbance of the mixture containing 5 mL 95% ethanol and 1 mL PDA NSs with different concentration, A_s is the absorbance of the mixture containing 5 mL DPPH and 1 mL PDA NSs with different concentration.

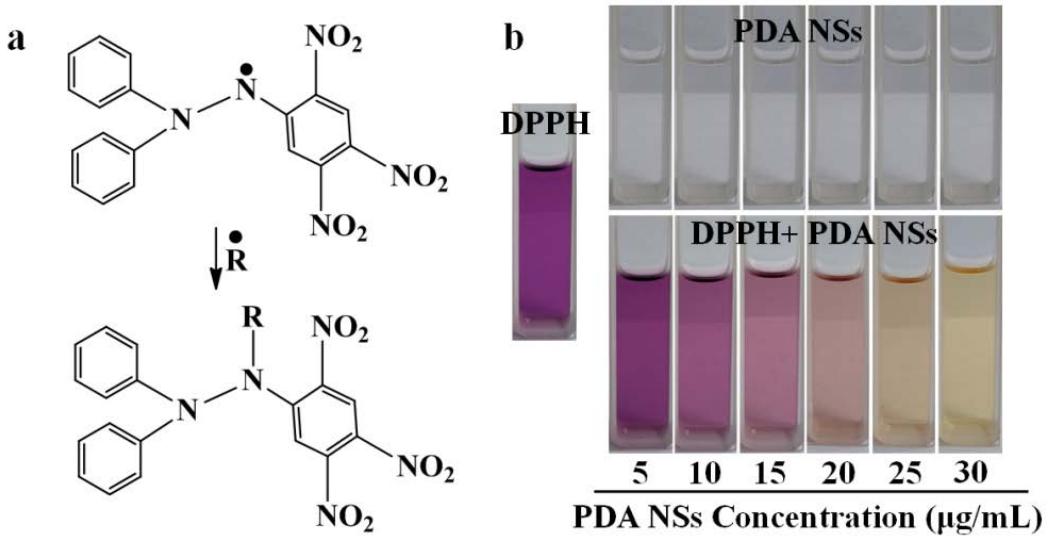

Figure S5. (a) The structure of DPPH· free radicals and the interaction principle with the scavenging agent. (b) Typical photographs of sample solutions (PDA NSs + DPPH) and control solutions (DPPH).

2.5 Scavenging of ABTS·$^+$

ABTS·$^+$ was first generated by the oxidation of ABTS with potassium sulfate ($K_2S_2O_8$). The blue-green ABTS·$^+$ solution was turned into colorless ABTS·H solution by adding antioxidants, indicating that ABTS free radicals had almost entirely disappeared.

The scavenging rate (Y) of ABTS·$^+$ free radical by PDA NSs was calculated according to Formula S3.

$$Y=(A_f-A_i) / A_f\times 100\% \quad (S3)$$

where A_f is the absorbance value of ABTS·$^+$ methanol solution, A_i is the absorbance of the mixture containing of ABTS·$^+$ and PDA NSs. All the absorbance was measureed at 745 nm.

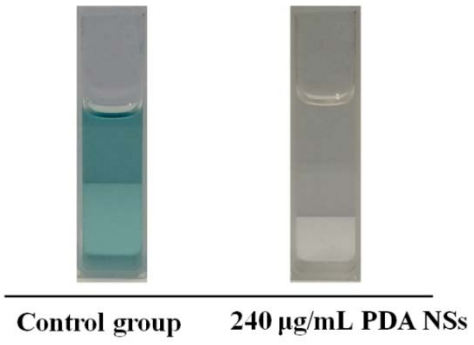

Figure S6. Typical photographs of ABTS·$^+$ sample solutions.

2.6 Cytotoxicity of PDA NSs for L929 mouse fibroblasts cells *in vitro*

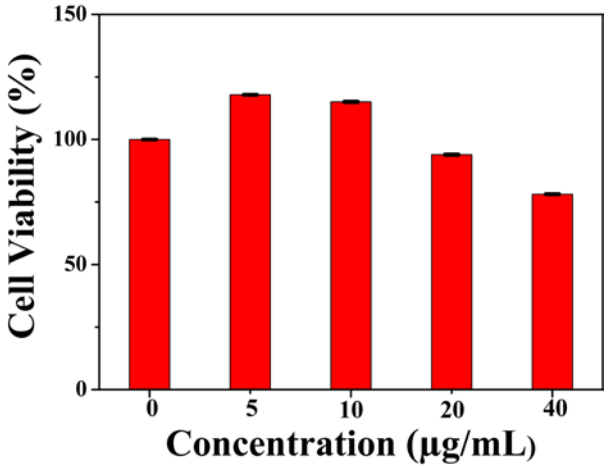

Figure S7. Different concentrations of PDA NSs solutions on L929 mouse fibroblasts cell viability after 24 h incubation.

2.7 Wound healing

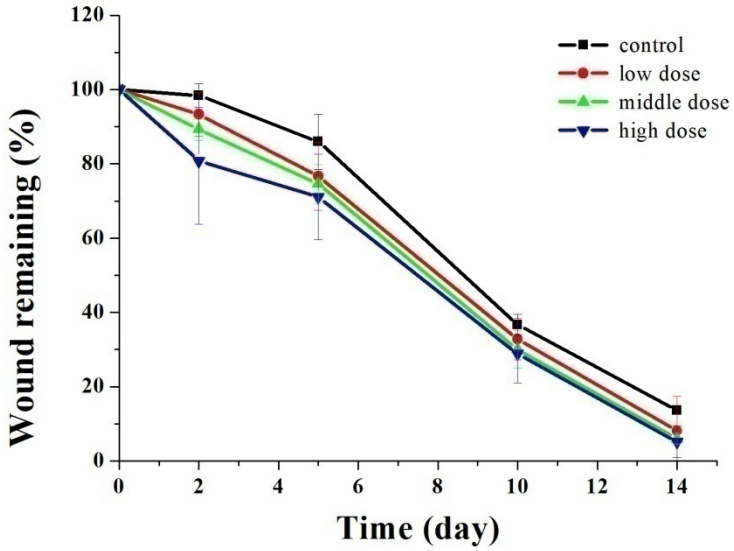

Figure S8 Unhealed wound of skin as a percentage of original wound, Mean ± SD, n=5.

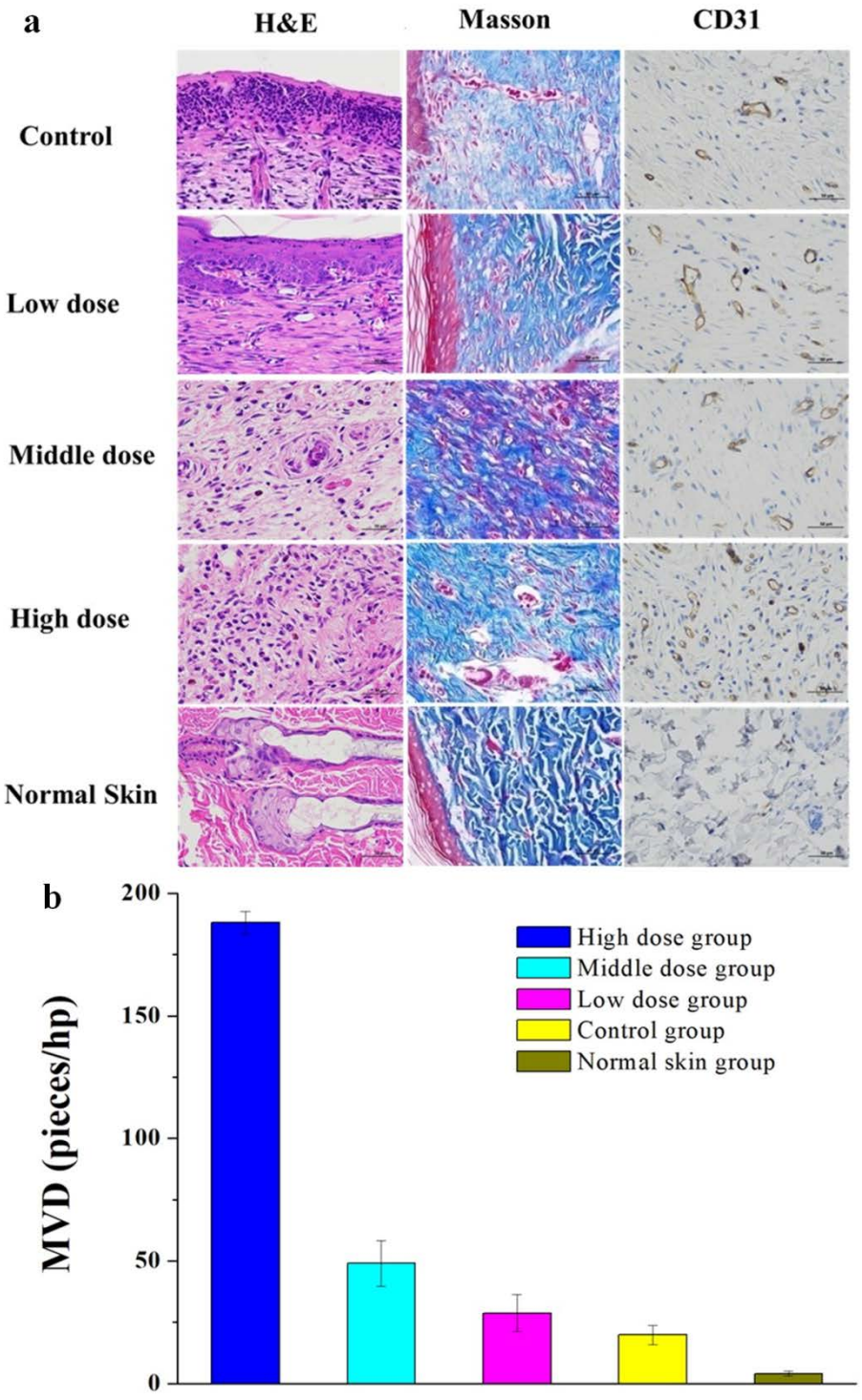

Figure S9. Histological and immunohistological analyses of rat skin tissue. (a) H&E (scale bars = 50 μm), Masson trichrome (scale bars = 500 μm), and CD 31 (scale bars = 50 μm) stained sections of granulation tissue; (b) Semiquantitative analysis of the microvessel density (MVD).

Notes and references

1 Y. L. Liu, K. L. Ai, J. H. Liu, M. Deng, Y. Y. He and L. H. Lu, Adv. Mater., 2013, 25, 1353–1359.

2 C. C. Ho and S. J. Ding, J. Mater. Sci.-Mater M., 24, 2381-2390.

3 P. J. Stephens, F. J. Devlin, C. F. Chabalowski and M. J. Frisch, J. Phys. Chem., 1994, 98, 11623.

4 W. J. Hehre, L. Radom, P. v. R. Schleyer and J. A. Pople, John Wiley & Sons: New York, 1987.

5 M. J. Frisch, G. W. Trucks, H. B. Schlegel, G. E. Scuseria, M. A. Robb, J. R. Cheeseman, G. Scalmani, V. Barone, B. Mennucci, G. A. Petersson, H. Nakatsuji, M. Caricato, X. Li, H. P. Hratchian, A. F. Izmaylov, J. Bloino, G. Zheng, J. L. Sonnenberg, M. Hada, M. Ehara, K. Toyota, R. Fukuda, J. Hasegawa, M. Ishida, T. Nakajima, Y. Honda, O. Kitao, H. Nakai, T. Vreven, J. A. Montgomery, Jr., J. E. Peralta, F. Ogliaro, M. Bearpark, J. J. Heyd, E. Brothers, K. N. Kudin, V. N. Staroverov, R. Kobayashi, J. Normand, K. Raghavachari, A. Rendell, J. C. Burant, S. S. Iyengar, J. Tomasi, M. Cossi, N. Rega, J. M. Millam, M. Klene, J. E. Knox, J. B. Cross, V. Bakken, C. Adamo, J. Jaramillo, R. Gomperts, R. E. Stratmann, O. Yazyev, A. J. Austin, R. Cammi, C. Pomelli, J. W. Ochterski, R. L. Martin, K. Morokuma, V. G. Zakrzewski, G. A. Voth, P. Salvador, J. J. Dannenberg, S. Dapprich, A. D. Daniels, Ö. Farkas, J. B. Foresman, J. V. Ortiz, J. Cioslowski, and D. J. Fox, Gaussian 09, Revision D.01; Gaussian, Inc., Wallingford CT, 2013.

6 J. J. P. Stewart, 2012 MOPAC2012 (Colorado Springs, CO, USA: Stewart Computational Chemistry).